

Supervised internal multi-model control of a dam-gallery open-channel system

E. Duviella, P. Charbonnaud, P. Chiron and F. J. Carrillo

Abstract— In this paper, a method for designing a supervised internal multi-model controller (SIMMC) is proposed. The structure is well-adapted for regulating non-linear plants for which some operating modes can be represented. A multimodeling method making possible to represent the operating modes is proposed. The supervision of the operating mode is carried out online and is combined with a control accommodation method which switches to the best controller. The considered plant is a dam-gallery open-channel system supplying a river with water and permitting all downstream uses. The effectiveness and the performances of the SIMMC are shown on a simulation of the plant using the real geometrical and physical data.

Keywords— Internal model control, internal multi-model control, switched control, supervised control.

I. INTRODUCTION

THE internal model control (IMC) concept was introduced in [9] as a general method which includes in its control structure a process model as an inherent part of the controller and the feedback is based on the difference between the outputs of the process and its model. This structure is appropriate for the design and implementation of controllers for open-loop stable systems. When the plant itself happens to be unknown, or the plant parameters vary slowly with time owing to ageing, no such model is directly available *a priori*, and one has to resort to identification techniques to come up with an appropriate plant model on-line. In [4], adaptation is combined with an IMC structure to obtain an adaptive IMC scheme possessing a theoretical proof. In [6], a class of minimum-phase input-output linearizable nonlinear systems with parameter uncertainty was controlled by an adaptive IMC. In [11] optimal closed-loop test design for IMC is studied. Closed-loop tests have operational advantages such as reduced disturbance and save operations, but it will also lead to better models for control. In [10]

Laboratoire Génie de Production, Ecole Nationale d'Ingénieurs de Tarbes, BP 1629, 65016 Tarbes Cedex, France, Phone: 33 5 62 44 27 34, fax: 33 5 62 44 27 08, e-mails: {Eric.Duviella|Philippe.Charbonnaud|Pascale.Chiron|carrillo}@enit.fr.

a reconfigurable adaptive control algorithm is proposed. The unknown autoregressive system dynamics are identified through a lattice filter which estimate the process reflection coefficients. The order of the system is inferred by monitoring the magnitude of the estimated reflection coefficients. The problem of control system design for time-delay systems has been solved for single input-single-output plants with a delay in the control input. The robust control of time-delay systems with both state and control delays was also addressed in [12] where an anisochronic extension of IMC was proposed. The system is called anisochronic because of non-synchronous role of state variables. A fuzzy relational model is a method from which a non linear system can be represented. In [5], a relational model from a fuzzy input space to a crisp output space is constructed by applying a least-squares identification technique to past process data. A method to determine its inverse model is proposed making possible to use the IMC structure.

Open channels systems are subjected to varying time delays. A robust design synthesis can be proposed to deal with modelling errors. In [7], an analytical modelling method based on physical equations of open-channel hydraulics is used, giving a nominal model and a bound on multiplicative uncertainties for a river reach. The robustness filter coefficients of the IMC are determined by a bisection algorithm, using μ -analysis for robustness requirements. The IMC is parametrized according to the main uncertainty, *i.e.* the time-delay, leaving only one design parameter.

In this paper, a supervised internal multi-model control (SIMMC) using prior knowledge of the system, is presented to carry out the regulation of a plant represented by a multimodel approach. In section II, the SIMMC structure is described and the design parameters are defined making possible to deal with parameter changes. The SIMMC is presented as an alternative to adaptive control methods. In section III, a dam-gallery open-channel system multi-modeling approach is detailed. In section IV, a supervised internal multi-model control of the

dam-gallery open-channel system is evaluated on a simulation of the plant using the real geometrical data. Finally, in section V, a conclusion highlights the effectiveness and performances of the SIMMC structure.

II. SUPERVISED INTERNAL MULTI-MODEL CONTROL

A multi-controller structure is required to control a plant with several Operating Modes (OM). Very often, the OM are well known. If not, they can be identified from the measured inputs and outputs. An analytical expression of the process output y can be approached as:

$$y \simeq \hat{y} = \sum_{j=1}^g \delta_m^j \cdot y_j, \quad (1)$$

where g is the number of plant operating modes, m denotes the actual operating mode, and δ_m^j is equal to 1 if $m = j$ and 0 otherwise. Each y_j is an estimate of the process output for a given control input u_r . The main problem of OM detection lies in the real-time estimation of m at the boundary between two OM, *i.e.*, the present behavior of the physical process in order to determine among a set of controllers the best fitted one. The aforementioned structure allows performing the plant mission in the presence of exogenous events p ([3]). The supervision set-point Σ describes the objectives, (e.g., change in the reference set-point, change in the control objective), to be achieved and the performances associated to the controller. The accommodation information vector α settles the set-points computed for the selected controller. The monitoring loop efficiency is linked to the detection time delay of an OM change given by the detection vector d . The accommodation strategy is selected according to the information vector compared to the supervision set-points. Before the next switching time, if the active controller does not allow achieving the performances for the given objective, the actual OM of the process must be identified to be accommodated by the right controller.

An active supervisory control of OM integrating an additional detection-accommodation loop is presented in Figure 1. This monitoring structure consists of two combined blocks, one for the model-based detection, Operating Mode Detection (OMD), which allows detecting a given process operating mode, and the other one for the control accommodation decision, Control Law Accommodation (CLA), which selects the right controller.

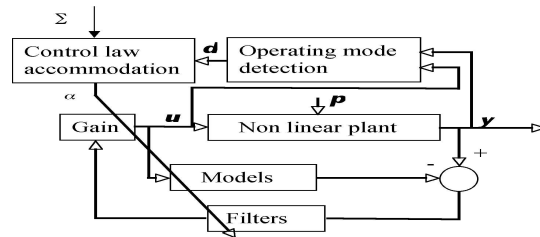


Fig. 1. Supervised internal multi-model controller.

Intuitively the notion of operating mode is linked to the tracking objective and also to its connected closed-loop performances. The fitted operating modes of a plant are always *a priori* well defined. When the OM are not *a priori* known the first step is to isolate the main operating modes and the second step is to identify the corresponding models. These modes induce a partition of the process model G of the plant P into a finite class of linear models $G = \{G_1, G_2, \dots, G_g\}$, where the i th linear model of the plant P is denoted G_i and $g = \text{card}(G)$, to which is associated a controller family C . The corresponding designed controller achieves the best performance of the closed-loop (C_i, G_i) . The controller C_i consists of a state gain, a process model and a filter.

In order to determine when and to which controller one should switch, a detection method is detailed in the following. The detector consists of three functions:

- the simulation of the models $G = \{G_j, j \in I\}$ controlled by the signal u_r which is the output of the active controller;
- the residue evaluation for each output model according to the fixed criterion;
- the function mode isolation based on the detection rule.

For each $j \in I$, the criterion is expressed by:

$$J_j(k) = \sum_{n=0}^{N-1} w_n \varepsilon_{j,n}(k), \quad (2)$$

where N is the size of the sliding window, $\varepsilon_{j,n}(k)$ is the j th identification error, $k > N$, and:

$$w_n = \frac{1}{N-1} \quad \text{and} \quad \varepsilon_{j,n}(k) = (y(k-n) - y_j(k-n))^2. \quad (3)$$

The multi-model output recursive square error criterion $J(k) = [J_1(k) \ J_2(k) \ \dots \ J_j(k) \ \dots]$ is computed with the recursive formula:

$$J_j(k) = J_j(k-1) + w_n(\varepsilon_j(k) - \varepsilon_j(k-N)). \quad (4)$$

The couple (d, t_d) defines the detection test which describes each OM detected $d(k)$ and the detection time $t_d(k)$:

The detection rule is computed on-line by:

$$d(k) = \{P = G_m, m = \arg \min_{1 \leq j \leq g} J_j(k)\}. \quad (5)$$

At each sampling period, a minimization of the criterion given by (2) is carried out to activate the controller corresponding to the model with the smallest index j . At the starting time, it is assumed that $d(0) = G_1$. The detection time is defined by:

$$t_d(k) = \{kT_d, d(k) \neq d(k-1)\}, \quad (6)$$

where T_d is the sampling period of the detection-accommodation loop. For a correct signal to noise ratio a good choice of N and T_d allows a good tuning of the multi-model based detector.

The accommodation block selects the adequate controller according to the supervision set-point Σ and to the detection vector d . The supervision set-point Σ is defined by the pair (O, Π^T) where O is the set of objectives to be achieved and $\Pi = [\pi_1, \pi_2, \dots, \pi_g]$ is the performance vector associated to the g modes, $\Pi \in \mathbb{R}^n$. In this paper, we consider only one objective, *i.e.*, tracking the output of a single-input single-output system to a constant reference input signal.

The accommodation vector α is a piecewise continuous switching signal which represents the series of the successive activated controllers. For the time kT_d , the activated controller is $C_{\alpha(k)}$, where the accommodation information vector α is expressed by:

$$\alpha(k) = \{l, [d(k) = G_l] \wedge [J_l < \pi_l]\}. \quad (7)$$

If the performance condition $J_l < \pi_l$ is not satisfied, an emergency shutdown procedure is activated and a maintenance operation is carried out on the damaged area of the system.

Let us consider the expression of the actual control input $u_r(k) = \sum_{i=1}^g \delta_{\alpha(k)}^i u_i$, $|u_i| < u_{\max}$.

III. DAM-GALLERY OPEN-CHANNEL SYSTEM MULTI-MODELING

The dam-gallery of Lunax-Save in french Pyrenees was built to supply with water the river Gesse. From a hollow jet valve, the water drains into an open-channel circular gallery, one kilometer long, before to supply the river. The steady discharge is obtained after more than one hour. Actuator dynamics are negligible.

Saint-Venant equations are accurately used with respect to the following assumptions: unidimensional discharge, the canal slope γ sufficiently weak to do the approximation: $\sin \gamma \simeq \gamma$, vertical accelerations are negligible. The diffusive wave equation (8), a simplified model of Saint-Venant equations, is preferred when the two following assumptions are verified: lateral discharges are null and inertia terms are negligible compared to one representing the energy lost by friction.

$$\frac{\partial Q(x,t)}{\partial t} + C(Q, z, x) \frac{\partial Q(x,t)}{\partial x} - D(Q, z, x) \frac{\partial^2 Q(x,t)}{\partial x^2} = 0, \quad (8)$$

where Q [m^3/s] is the discharge, z [m] is the absolute water surface elevation and x [m] is the reach length, with a celerity C [m/s] and a diffusion D [m^2/s]:

$$\begin{cases} C(Q, z, x) = \frac{1}{L^2 \frac{\partial f_s}{\partial Q}} \left[\frac{\partial L}{\partial x} - \frac{\partial(Lf_s)}{\partial z} \right], \\ D(Q, z, x) = \frac{1}{L} \frac{\partial f_s}{\partial Q}, \end{cases} \quad (9)$$

where L is the water surface width and f_s is the friction slope. Hayami equation is obtained by linearizing (8) for a reference discharge Q_e :

$$\frac{\partial q(x,t)}{\partial t} + C_e \frac{\partial q(x,t)}{\partial x} - D_e \frac{\partial^2 q(x,t)}{\partial x^2} = 0. \quad (10)$$

where $Q = Q_e + q$. The discharge variation q from the reference discharge Q_e is drained with a mean speed of constant celerity C_e and is diffused with a constant diffusion coefficient D_e . As discussed in [8], the Hayami transfer function linking the upstream discharge $Q_{up}(s)$ to the downstream discharge $Q_{down}(x, s)$ for a reach of length x can be derived from the Hayami equation (10) and is expressed by:

$$F(x, s) = e^{\frac{x C_e}{2 D_e} \left(1 - \sqrt{1 + 4 \frac{D_e}{C_e^2} s} \right)}. \quad (11)$$

The moment matching method detailed in [8] is used to identify (11) to a second order transfer function with delay:

$$F(s) = \frac{b_1 e^{-s\tau}}{1 + a_1 s + a_2 s^2}, \quad (12)$$

where the transfer parameters can be written as detailed in [1]:

$$\begin{cases} b_1 = 1, \\ a_1 = (-d + \sqrt{\Delta})^{1/3} + (-d - \sqrt{\Delta})^{1/3}, \\ a_2 = \frac{2x D_e}{C_e^3} \left(1 - 3 \frac{D_e}{a_1 C_e^2} \right), \\ \tau = \frac{x}{C_e} - a_1, \end{cases} \quad (13)$$

$$\text{with } d = \frac{6xD_e^2}{C_e^5} \text{ and } \Delta = \frac{4x^2D_e^3}{C_e^9} \left(\frac{9D_e}{C_e} - 2x \right).$$

In the case of a circular profile, from the absolute water surface elevation z and the radius R [m], the angle θ [rad], the water surface width L [m], the wetted area S [m²] and the wetted perimeter P [m] have been expressed by:

$$\begin{cases} \theta = 2 \arccos \left(\frac{z-R}{R} \right), \\ L = 2\sqrt{2Rz - z^2}, \\ S = \pi R^2 + L \frac{z-R}{2} - \frac{1}{2} R^2 \theta, \\ P = 2\pi R - R\theta. \end{cases} \quad (14)$$

For $f_s = \gamma$, frictions are modelled by the Manning-Strickler formula:

$$f_s = \frac{Q^2 n^2}{S^2 R_h^{4/3}} = \gamma, \quad (15)$$

where n is the Manning coefficient and R_h the hydraulic radius corresponding to the wetted surface S divided by the wetted perimeter P .

In fact, only three parameters z , R and γ are sufficient for defining the four others. For an open-channel system with a circular profile, coefficients C_e and D_e defined by (9) are finally calculated as:

$$\begin{cases} C_e = \frac{Q_e}{L^2} \left(-\frac{2(R-z)}{L} + \frac{1}{3P} \left(5\frac{P}{S} \left(\frac{L^2}{2} + 4Rz - 2z^2 \right) - 8R \right) \right), \\ D_e = \frac{Q_e}{2Lf_s}. \end{cases} \quad (16)$$

The gallery dynamics was modelled by a multi-modeling approach. Each model is a second order with delay (12), and the values of the corresponding parameters a_1 , a_2 and τ must be calculated. Combining relations (14) and (15), the equation (17) makes possible to determine, numerically, the water elevation z according to Q , then, according to the equations (16), to calculate the coefficients C_e and D_e . Finally, the coefficients a_1 , a_2 and τ can be computed by relation (13).

$$\frac{f_s}{Q^2 n^2} = \frac{\left(2R \arccos \left(\frac{R-z}{R} \right) \right)^{4/3}}{\left((z-R) \sqrt{2Rz - z^2} + R^2 \arccos \left(\frac{R-z}{R} \right) \right)^{10/3}}. \quad (17)$$

According to the geometrical data of the gallery, *i.e.* the radius $R = 0.9$ m, the length $x = 946.65$ m, the slope $\gamma = 0.0026$ rad and the Manning coefficient $n = 0.015$, and to the operating range of the gallery discharge, *i.e.* $Q \in [0.5; 5]$, it was possible to determine the value of each parameter according to each discharge Q_e , *i.e.* 0.75, 1.5, 2.8 and 4.4 m³/s. In order to reduce the number of models, we consider to accept as correct a model for which a

$[Q_{\text{inf}_i}; Q_{\text{sup}_i}[$	a_1	a_2	τ
$[0, 1[$	245	17360	252
$[1, 2[$	234	15050	173
$[2, 3.6[$	222	12310	110
$[3.6, 5]$	199	8396	73

TABLE I
TRANSFER FUNCTION PARAMETERS ACCORDING TO THE
DISCHARGE AREA.

predefined error is allowed on the value of the parameters. The number of models and the discharge intervals are selected according to a percentage of error Π_C on the celerity C_e . The operating range is decomposed starting with the median celerity C_{med} (18) which is calculated from the minimum C_{min} and the maximum C_{max} celerities corresponding to, respectively, the maximum Q_{max} and the minimum Q_{min} discharges. For each obtained model i , a validity interval $[C_{\text{inf}_i}; C_{\text{sup}_i}[$ is calculated according to Π_C , and a celerity, denoted C_i , which corresponds to the center of the interval is computed.

$$C_{\text{med}} = \frac{C_{\text{max}} + C_{\text{min}}}{2}. \quad (18)$$

Relation (19), obtained from relations (15) and (16), is numerically solved with a resolution of one millimeter, to determine the absolute water surface elevation z_i for the interval $[C_{\text{inf}_i}; C_{\text{sup}_i}[$ according to the value of C_i .

$$C_i = \frac{\sqrt{f_s} S^{5/3}}{nP^{2/3} L^2} \left(-\frac{2(R-z_i)}{L} + \frac{1}{3P} \left(5\frac{P}{S} \left(\frac{L^2}{2} + 4Rz_i - 2z_i^2 \right) - 8R \right) \right), \quad (19)$$

where the parameters L , P and S are expressed according to the geometrical data of plant and z_i . From z_i the discharge Q_{e_i} and the coefficient D_i are calculated. The limits of the interval $[Q_{\text{inf}_i}; Q_{\text{sup}_i}[$ of each model i is determined according to the same principle for the celerities C_{inf_i} and C_{sup_i} . The modelization of the gallery is carried out according to a percentage of error $\Pi_C = 15$ %. From the value of water elevation z and with the values of C_e and D_e given by (16), parameters a_0 , a_1 and τ are calculated. In Table I, analytically identification results of the second order transfer with delay are displayed for the considered discharge intervals.

IV. SUPERVISED INTERNAL MULTI-MODEL CONTROLS OF THE DAM-GALLERY OPEN-CHANNEL SYSTEM

The SIMMC designed for the dam-gallery open channel system, was implemented in the usual form presented in [9] (see Figure 2). The detection vector d resulting to the Operating Mode Detection block (OMD), is determined according to a size of the sliding window $N = 4$. In the Control Law Accommodation block (CLA), the selection α of the best controller is carried out according to d and the performance conditions $\pi_i = 3, i = 1, \dots, 4$. Due to the process dynamics, there is no significant bump in the control u_r . Otherwise, AntiWindup Bumpless Transfer (AWBT) compensators can be introduced as proposed in [3]. The set-point resulting from CLA, is the discharge q_{M1obj} . The control u_r which corresponds to the upstream discharge, is sent to the non-linear plant which provides the downstream discharge q_{M1} . The non-linear plant simulation is carried out by the Simulation of Irrigation Canals (SIC) software, which solves the Saint Venant equations using the Preissmann's scheme [2]. The gallery was modelled with SIC according to its geometrical data. The input of the SIC model of the gallery is the upstream discharge u_r and the output is the downstream discharge q_{M1} .

Continuous models $F_i(s)$ identified according to the multi-modelling method (see Tab.I) were discretized at the control period $T_c = 60$ s, giving four discretized models $G_{i c}$:

$$G_{i c} = \frac{B_i(z^{-1})}{A_i(z^{-1})}. \quad (20)$$

The detection period was chosen $T_d = \frac{T_c}{5} = 12$ s. The stability of SIMMC depends on the choice of stable filter $f_{i c}$:

$$f_{i c} = \frac{(1 - \beta)z^{-1}}{1 - \beta z^{-1}}. \quad (21)$$

For the evaluation of the SIMMC, the transfer $H_{i c}$ corresponds to the static gain of the inverse process model; $H_{i c} = 1$. The performances are linked to the SIMMC parameter tuning. Coefficient β tuned at 0.8, by simulation, leads to a good compromise between performance and robustness of the closed loop.

In Figure 3.d, the set-point q_{M1obj} is presented in continuous line. The downstream discharge measurement q_{M1} is subjected to disturbances with noise of $0.2 \text{ m}^3/\text{s}$ from $t = 50 \text{ min}$, of $0.3 \text{ m}^3/\text{s}$ from

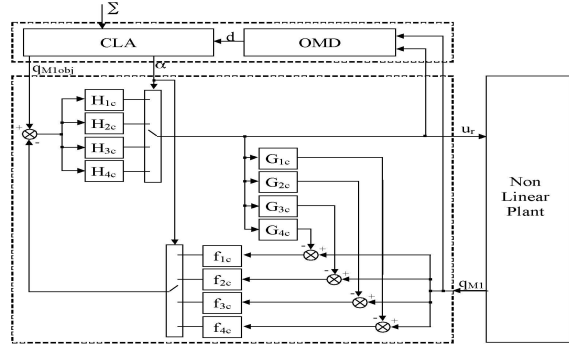


Fig. 2. SIMMC structure.

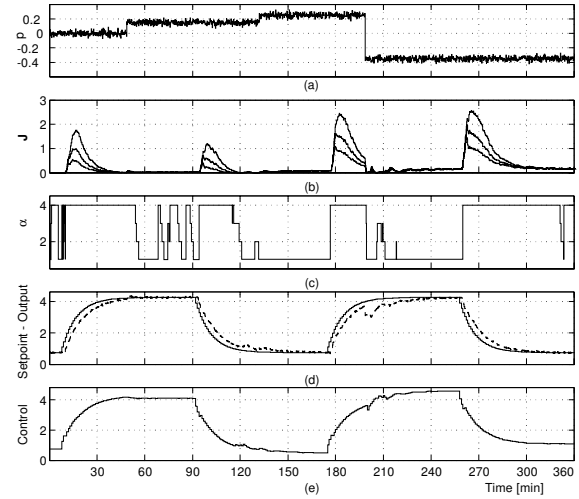


Fig. 3. SIMMC results (a) perturbation p , (b) criteria J , (c) accommodation signal α , (d) setpoint q_{M1obj} and output q_{M1} , (e) effective control u_r .

$t = 130 \text{ min}$, and of $-0.4 \text{ m}^3/\text{s}$ from $t = 200 \text{ min}$ (see Figure 3.a). The measurement noise has a variance of 0.01. The computation of criterion J presented in Figure 3.b, allows the selection α of the model (see Figure 3.c). The effective control u_r is depicted in Figure 3.e. In Figure 3.d, the measured downstream discharge q_{M_i} is displayed in dashed line. The SIMMC control is robust with the disturbances and the downstream discharge is close to the set-point.

In order to evaluate the performances of the SIMMC regulation, a digital PID controller sampled at T_c was also designed. The integral action carried out on the error between the set-point and the output, *i.e.* downstream discharge, the proportional and derivative actions are carried out on the output only. Coefficients K_P , K_I and K_D are computed

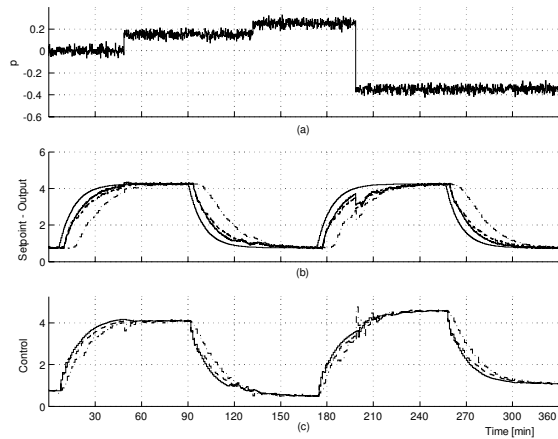


Fig. 4. PID (dotted line), IMC (dashed line) and SIMMC (continuous line) comparison for a (a) perturbation p , (b) a setpoint $q_{M_i obj}$ and corresponding outputs q_{M_i} , (c) and their effective controls u_r .

by a Takahashi step response method for the model identified around $1.5 \text{ m}^3/\text{s}$. The values of the coefficients are $K_P = 0.83$, $K_I = 0.11$ and $K_D = 1.85$:

$$u_{PID} = -K_P y_k + \frac{K_I}{1 - z^{-1}} E_k - K_D(1 - z^{-1})y_k, \quad (22)$$

and $E_k = cons_k - y_k$, where $cons_k$ is the set-point which corresponds to $q_{M_1 obj k}$ and y_k the output, *i.e.* q_{M_i} .

On the other hand, an IMC based on the model identified around $1.5 \text{ m}^3/\text{s}$ is proposed. The two controllers are tested on the same scenario of set-point and disturbances. The PID, IMC and SIMMC regulations are depicted respectively in dashed-dotted line, in dashed line and in continuous line in Figure 4.c. The downstream discharge is depicted according to same convention in Figure 4.b. The PID controller is not robust to the noise and the disturbances; its performances are not so good. The IMC is slower than the SIMMC. The performances of the controllers are evaluated on a criterion of volume in lack or in excess during 6 hours. The SIMMC is the better one with a volume in lack or in excess of 4630 m^3 compared to the IMC with a volume of 6055 m^3 and to the PID controller with a volume of 14222 m^3 . The SIMMC provides thus an economy of 1425 m^3 compared to IMC and of 9592 m^3 compared to the PID.

V. CONCLUSION

A method for designing a supervised internal multi-model controller was detailed. The structure

is well-adapted for regulating non-linear plants for which some operating modes can be represented. A multimodeling method making possible to represent the operating modes was proposed and applied to the considered plant which is a dam-gallery open-channel system supplying a river with water and permitting all downstream uses. The supervision of the operating mode is carried out online and is combined with a control accommodation method which switches to the best controller. The effectiveness and the performances of the SIMMC are shown on a simulation of the plant using the real geometrical and physical data. The resulting water volume economy is significant.

Acknowledgement This work was supported by the Communauté de Travail des Pyrénées referenced as the GERHYCO project n°02008962 by the Conseil Régional de Midi-Pyrénées. Thanks also to our partner the CACG company and its engineering department, located at Tarbes (France).

REFERENCES

- [1] J.-P. Baume, J. Sau and P.-O. Malaterre. Modelling of irrigation channel dynamics for controller design. IEEE International Conference on Systems, Man, and Cybernetics, vol.4, pp. 3856-3861, San Diego, USA, 1998.
- [2] CEMAGREF. SIC user's guide and theoretical concepts. Montpellier, 1992.
- [3] P. Charbonnaud, F. Rotella et S. Médar. Process Operating Mode Monitoring: Switching Online the Right Controller, IEEE Transactions on Systems, Man and Cybernetics, Part C, vol.31, n°1, pp. 77-86, February 2001.
- [4] A. Datta and J. Ochoa. Adaptive internal model control: Design and stability analysis. Automatica, vol. 32, Issue 2, pp. 261-266, February 1996.
- [5] C. R. Edgar and B. E. Postlethwaite. MIMO fuzzy internal model control. Automatica, vol. 36, Issue 6, pp. 867-877, June 2000.
- [6] Q. Hu and G. P. Rangaiah. Adaptive internal model control of nonlinear processes. Chemical Engineering Science, vol. 54, Issue 9, pp. 1205-1220, May 1999.
- [7] X. Litrico. Robust IMC flow control of SIMO Dam-River Open-Channel Systems. IEEE Transactions on control systems technology, vol. 10, N°3, May 2002.
- [8] X. Litrico and D. Georges. Robust continuous-time and discrete-time flow control of a dam river system. (I) Modelling. Applied Mathematical Modelling, vol. 23, pp. 809-827, 1999.
- [9] M. Morari and E. Zafriou. Robust process control. PTR Prentice Hall Englewood Cliffs, New Jersey, 1989.
- [10] G. Nikolakopoulos and A. Tzes. Reconfigurable internal model control based on adaptive lattice filtering. Mathematics and Computers in Simulation, vol. 60, Issues 3-5, pp. 303-314, 30 September 2002.
- [11] Y. Zhu and P. P. J. van den Bosch. Optimal closed-loop identification test design for internal model control. Automatica, vol. 36, Issue 8, pp. 1237-1241, August 2000.
- [12] P. Zitek and J. Hlava. Anisochronic internal model control of time-delay systems. Control Engineering Practice, vol. 9, Issue 5, pp. 501-516, May 2001.